



ELSEVIER

Surface Science 397 (1998) L273–L279

surface science

Surface Science Letters

Real-time scanning tunneling microscopy observation of Si(100)-(2 × 1) → (2 × n) → c(4 × 4) structural phase transitions

Deng-Sung Lin *, Perng-Horng Wu

Institute of Physics, National Chiao-Tung University, 75 Bo-Ai Street, Hsinchu 300, Taiwan

Received 18 July 1997; accepted for publication 5 November 1997

Abstract

We report on the discovery of Si(100)-(2 × 1) → (2 × n) → c(4 × 4) structural phase transitions. Annealing the Si(100)-(2 × 1) surface between 590 and 700°C for some hours causes dimer vacancies to increase and nucleate into chains, ultimately forming the (2 × n) structure. After further annealing, c(4 × 4) areas appear, grow, and finally cover the entire surface. Experimental results raise the possibility not only that c(4 × 4) is a stable low-temperature structure of Si(100), but that (2 × 1) is a high-temperature phase stabilized at room temperature owing to its kinetic limitations. © 1998 Elsevier Science B.V.

Keywords: Scanning tunneling microscopy, Silicon, Surface thermodynamics

A more thorough understanding of surface atomic structures is essential to research involving surface, interface, and thin film science and technology. The Si(100) surface has been widely investigated owing to its relevance in fundamental science as well as Si integrated circuit technology [1,2]. The clean Si(100) surface typically displays a two-domain (2 × 1) reconstruction caused by the formation of dimers which are arranged in parallel rows. The preparation procedure for the (2 × 1) structure includes ~1200°C annealing and typical cooling rates of $\geq 1^\circ\text{C s}^{-1}$. Interestingly, the Si(100)-(2 × 1) surface consistently contains a small percentage of dimer vacancies (DVs) and vacancy clusters [2–4]. Moreover, several investigations have noted that rapid thermal quenching

[5–8], annealing after Ar⁺ bombardment [9], thermal desorption of oxide layers [10,11] and homoepitaxial growth contribute to the formation of the (2 × n) ($6 \leq n \leq 12$) defect structure on Si(100) [12–14]. Although metal (particularly Ni) contamination clearly leads to the (2 × n) structure [15], the above experiments found little trace of Ni in their samples. This finding implies that the (2 × n) ordering is most probably governed by some mechanism which does not require Ni [6,16].

In addition, the several preparation techniques used to observe a c(4 × 4) reconstruction include (i) keeping the Si(100)-(2 × 1) surface at 600°C for 5 min [17], (ii) growing Si on Si(100)-(2 × 1) at 600–750°C by molecular-beam epitaxy [12,18,19] or chemical vapor deposition [13,20,21], (iii) annealing H-covered Si(100) at 570–690°C [22,23], (iv) exposing Si(100)-(2 × 1) to O₂ at RT followed by annealing at 600–650°C

* Corresponding author. Fax (+886) 3 5720728, e-mail: dslin@cc.nctu.edu.tw

[10,24], and (v) exposing Si(100) to C_2H_4 at 5×10^{-6} Torr for 5 min at $600^\circ C$ [25]. These techniques employ various gases or molecular beams free of metallic contamination on samples with various bulk impurities. However, STM investigations revealed exactly the same $c(4 \times 4)$ atomic arrangement [10,13,14,22,23]. These investigators obtained the $c(4 \times 4)$ reconstruction via unique surface treatments and converted it back to (2×1) by annealing at $\geq 750^\circ C$, thereby assuming it to be metastable. Interestingly, $(2 \times n)$ and $c(4 \times 4)$ phases coexist on the Si(100) surfaces after complete desorption of thin oxide layers or homoepitaxy [10,12,13]. Nevertheless, despite such extensive studies, no consensus regarding the formation mechanisms of $(2 \times n)$ and $c(4 \times 4)$ has been reached.

This work demonstrates that the (2×1) reconstruction on Si(100) undergoes phase transitions to the $c(4 \times 4)$ structure via an intermediate $(2 \times n)$ phase after prolonged annealing at 590 – $700^\circ C$. Around 6, 34 and 220 h are necessary to complete the structural transformations for annealing temperatures of 700, 650 and $590^\circ C$, respectively. Such an unexpectedly long relaxation time caused these transitions to be overlooked previously. Furthermore, annealing the $c(4 \times 4)$ surface at $760^\circ C$ for ~ 10 s recovers the (2×1) structure. The above observations strongly suggest not only that $(2 \times n)$ and $c(4 \times 4)$ are intrinsic structures of Si(100), but also that (2×1) is a high-temperature phase. Consequently, the (2×1) reconstruction is typically obtained at RT owing to its kinetic limitations during quenching. Such findings not only necessitate a re-examination of previous works concerning Si(100), but are also of significance to the development of various low-temperature processes on this surface.

The experiments reported here were performed in a vacuum chamber with a base pressure of 7×10^{-11} Torr, using an Omicron variable-temperature STM. The Si(100) samples (B-doped, $10 \Omega \cdot cm$, Wacker) were mounted on holders made of Ta, Mo and ZrO ceramic plates. The starting Si(100)- (2×1) surfaces were prepared by direct Joule heating at $\sim 1200^\circ C$ with subsequent radiation quenching. The sample temperature was measured by an infrared pyrometer.

Fig. 1 illustrates the structural phase transition experiment. In this study, a clean Si(100)- (2×1) surface with a low concentration of DVs was heated and kept at $590^\circ C$ for 0.5, 9.5, 33, 54, 100, 140 and 220 h (Figs. 1a–g, respectively). During the experiment, the tip was moved around in a range of ~ 1 mm in diameter to confirm that global transitions had occurred on the surface. The primary features in Fig. 1a denote alternate terraces with (2×1) and (1×2) periodicities, separated by two types of steps (S_A and S_B). After 0.5 h annealing, more DVs and vacancy clusters (appearing as dark spots and short lines) became visible on the smooth terraces in Fig. 1a. Presumably, the initial DVs, frozen in from high temperatures by quenching, reduce their population as the sample is annealed, provided that their formation energies are positive [4]. However, increasing the annealing time causes more DVs to be generated thermally. At this temperature, Fig. 1b reveals that DVs can move around, causing individual DVs to nucleate into short lines. The ordering of DVs is driven by the DV–DV interaction [4,6]. After further annealing, as shown in Fig. 1c, the VLs grow in length and their density increases. The VLs, which strongly repel each other, are regularly spaced and form $(2 \times n)$ (on average $n \approx 11$) reconstruction.

Further annealing does not alter the $(2 \times n)$ structure's overall features. However, as Fig. 1d indicates, small areas with $c(4 \times 4)$ symmetry start condensing around the steps and on the middle of $(2 \times n)$ domains. The $c(4 \times 4)$ regions have a lower average apparent height than the surrounding $(2 \times n)$ domains due to both topographical and electronic effects [12], and therefore appear as darker areas in the images. As Figs. 1d–g reveal, the $c(4 \times 4)$ regions grow in size over time, eventually covering the entire surface (Fig. 1g). The total annealing time taken to complete the $(2 \times 1) \rightarrow (2 \times n) \rightarrow c(4 \times 4)$ transitions at $590^\circ C$ is 220 h. The same transition process takes roughly 34 and 6 h for annealing temperatures of 650 and $700^\circ C$, respectively. When the annealing temperature exceeds $700^\circ C$, three-dimensional (3D) islands gradually form on the surfaces during the formation of the $c(4 \times 4)$ phase. As Fig. 2 shows, annealing a surface such as that in Fig. 1g at $760^\circ C$ for only ~ 10 s causes the $c(4 \times 4)$ structure to trans-

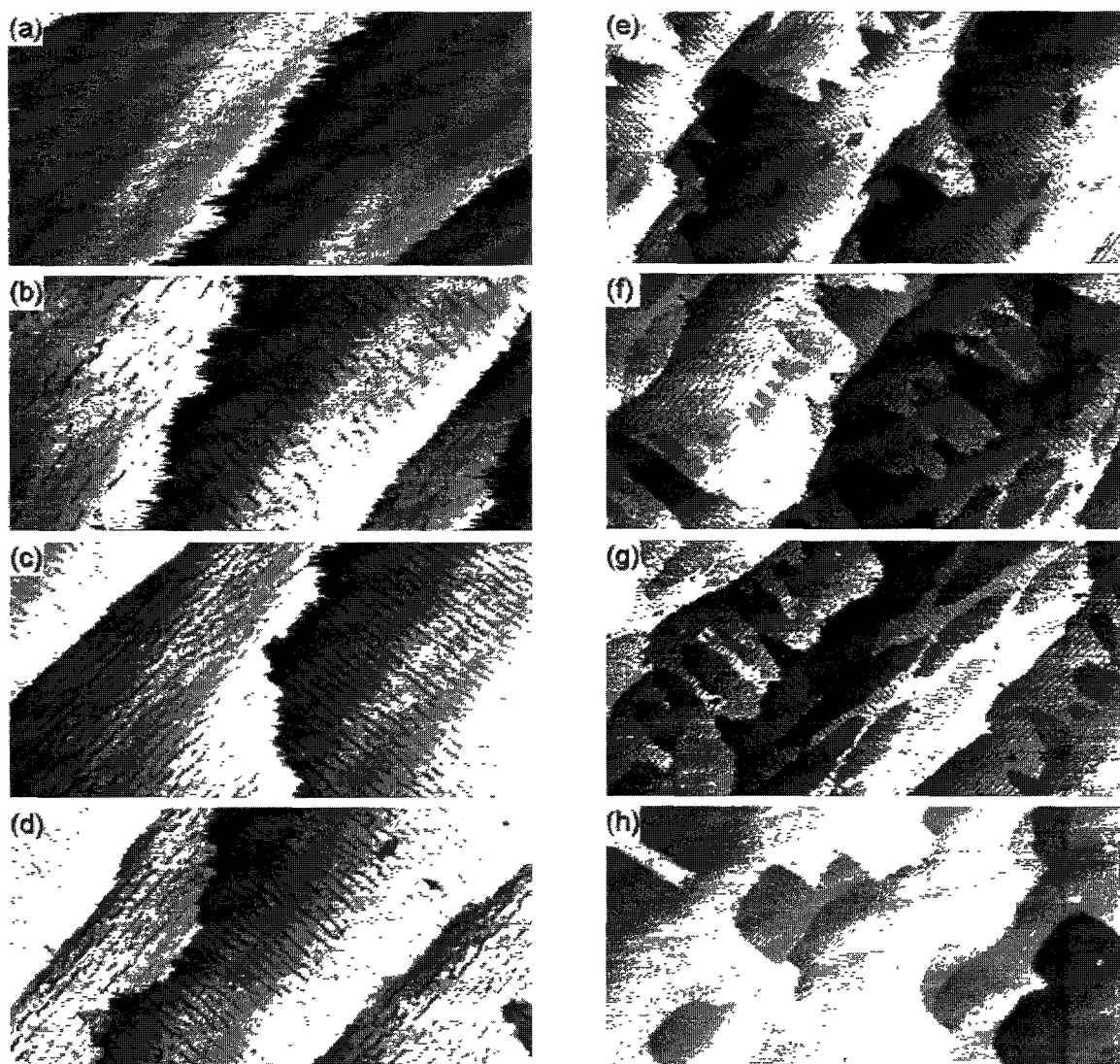


Fig. 1. STM images obtained in real time after a clean Si(100)-(2 \times 1) surface was kept at 590°C for (a) 0.5, (b) 9.5, (c) 33, (d) 54, (e) 100, (f) 140 and (g) 220 h. The tip bias (V_T) was 2.0 V. The image sizes are 2000 Å \times 1000 Å for (a)–(c) and 4000 Å \times 2000 Å for (d)–(g). (a)–(c) depict the transition (2 \times 1) \rightarrow (2 \times n), and (d)–(g) the transition (2 \times n) \rightarrow c(4 \times 4).

form back to (2 \times 1). 3D islands also form. At 760°C, rapid thermal motion of surface atoms and steps occurs, leading to noisy STM images. Therefore, the surface roughening in three dimensions and the simultaneous deconstruction of c(4 \times 4) probably result in the disappearance of the step free energy of the c(4 \times 4) structure at this temperature [26].

According to Figs. 3a and b, the atomic features of the c(4 \times 4) structure resemble those prepared via O₂, H, Si₂H₆ and Si molecular-beam exposure [10, 12, 13, 22, 23]. Furthermore, previous investigations have verified that Si(100)-c(4 \times 4) corresponds to a contamination-free surface [10, 12, 17, 22–24]. Therefore, our data closely correspond to a nominal 50/50 mosaic mixture of the parallel

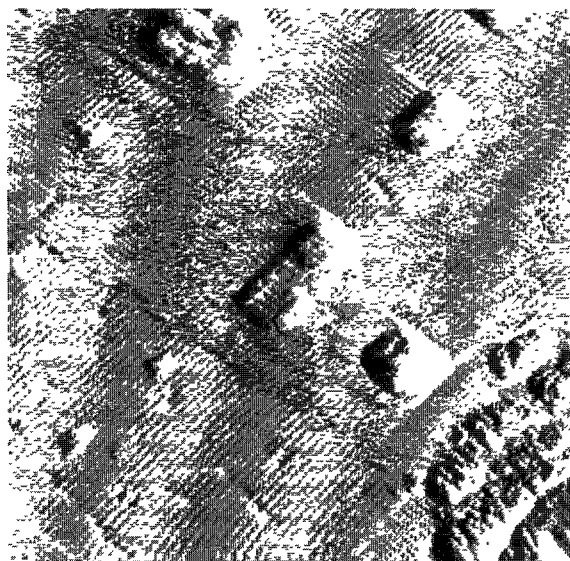


Fig. 2 STM image ($\sim 545 \text{ \AA} \times 545 \text{ \AA}$) taken at 590°C after annealing the Si(100)- $c(4 \times 4)$ surface at 760°C for $\sim 10 \text{ s}$. The image has been differentiated to illustrate the monatomic steps and 3D islands.

ad-dimer and mixed ad-dimer structures established by Uhrberg et al. [22]. Although diborane exposure leads to the formation of $c(4 \times 4)$ patches [27], the $c(4 \times 4)$ structure cannot be obtained by extended high-temperature annealing of B-doped Si(100) samples [28]. To address further the question of contamination, Fig. 4 presents the STM-tip induced conversion of the $c(4 \times 4)$ reconstruction on Si(100)- (2×1) by repeated scanning over the same area (aside from thermal drifts) at a higher tip bias ($+2.6 \text{ V}$). In this study, the images were taken at 90 s intervals after the Si(100) surface had been kept at 650°C for $\sim 0.5 \text{ h}$ (essentially, the surface remains (2×1) -reconstructed). (The $c(4 \times 4)$ structure is similarly converted for the $(2 \times n)$ structure after annealing for 6 h.) After the tip is moved to a new area, the initial scan (Fig. 4a) shows only smooth terraces. As shown in Figs. 4b–e, subsequent scans reveal the increasing condensation of darker $c(4 \times 4)$ regions. While the exact conversion mechanism remains unclear (as discussed below), the generation of $c(4 \times 4)$ is clearly associated with local tip–surface interactions. Such interactions are evident because the $c(4 \times 4)$ areas appear only in the center region on

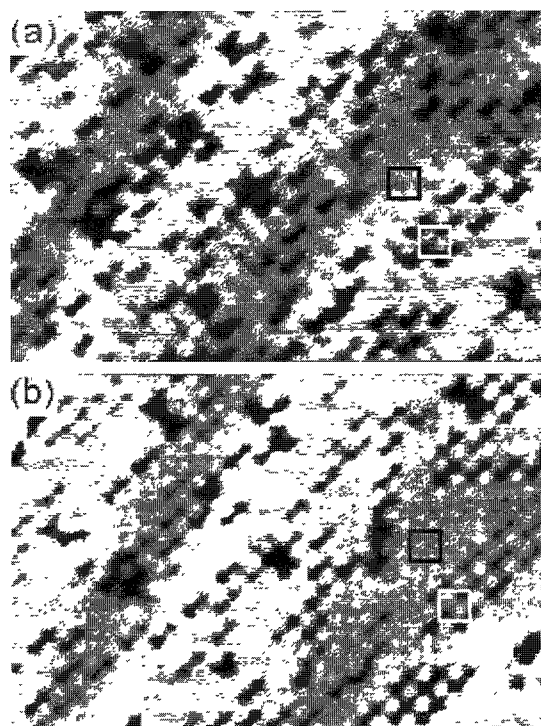


Fig. 3 Dual-voltage STM images ($\sim 174 \text{ \AA} \times 115 \text{ \AA}$) of Si(100)- $c(4 \times 4)$ taken at RT at (a) $V_t = 2.0 \text{ V}$ and (b) $V_t = -2.0 \text{ V}$. Following the atomic models in Ref. [22], the black and white squares outline $c(4 \times 4)$ primitive cells of the mixed ad-dimer and parallel ad-dimer structures, respectively.

the first scan (Fig. 4f) over a zoom-out area. Moreover, brief annealing at 760°C converts the $c(4 \times 4)$ pattern back to (2×1) . Although the $(2 \times 1) \rightarrow (2 \times n) \rightarrow c(4 \times 4)$ transitions caused by thermal activation take 34 h at 650°C , the tip-induced conversion to $c(4 \times 4)$ takes only a few minutes. Therefore, the effects of adsorption and/or etching by residual background gases such as O_2 and H_2 , metal contaminations from the sample holder, and bulk impurity diffusion during the formation of the $c(4 \times 4)$ phase can be ruled out [29]. The possibility exists that the STM tip deposits W during scanning. However, the same $c(4 \times 4)$ pattern is observed, and can be converted back to (2×1) at the same temperature. These findings strongly suggest that $c(4 \times 4)$ is an intrinsic structure, in that different contaminations are unlikely to generate the same atomic arrangement and have the same conversion temperature.

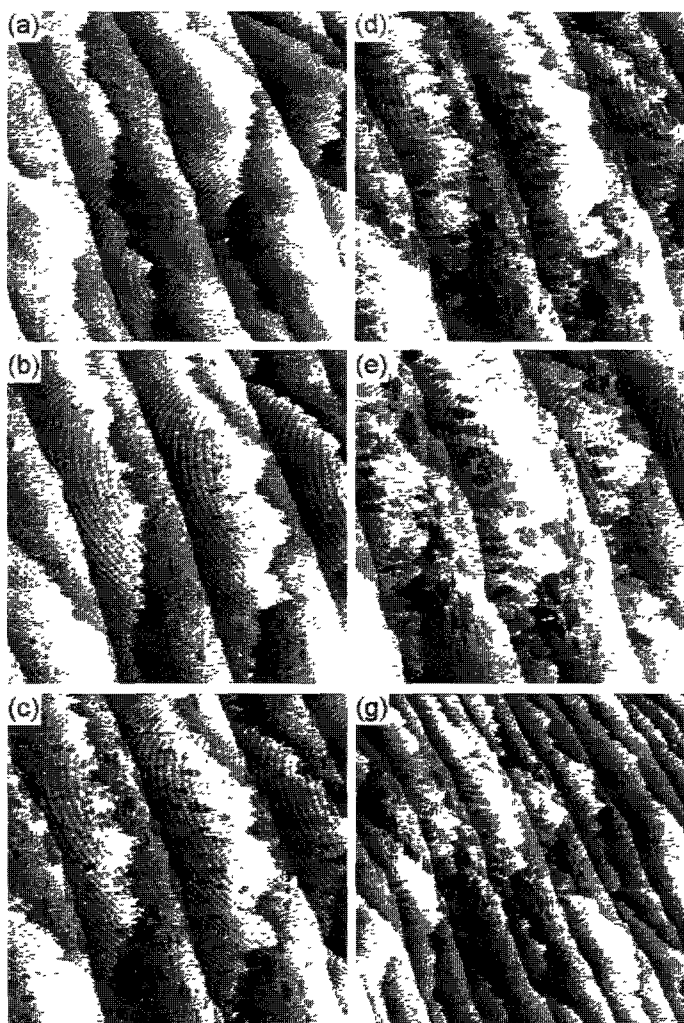


Fig 4 STM-tip activated formation of the local $c(4 \times 4)$ structure at 650°C on $\text{Si}(100)-(2 \times 1)$. The six images were obtained consecutively. Each image took 90 s to acquire at $V_t = +2.6$ V and $I_t = 0.25$ nA. The scan size is $0.5 \mu\text{m} \times 0.5 \mu\text{m}$ for (a)–(e) and $1 \mu\text{m} \times 1 \mu\text{m}$ for (f). The Moiré pattern (resulting from an interference of the lattice spacing and data point density) is only visible on every second terrace because the alternating (1×2) and (2×1) domains have a different atomic spacing in the scanning direction. Thermal drift in the upper-left direction can be observed.

The change in surface morphology from the (2×1) phase to $(2 \times n)$ is not abrupt. The DV concentration rises smoothly and homogeneously during the $(2 \times 1) \rightarrow (2 \times n)$ transition. In contrast, the $(2 \times n) \rightarrow c(4 \times 4)$ transition behaves quite differently. Close examination of Figs. 1d and 1e reveals that (i) the transition exhibits the familiar phenomena of phase coexistence and nucleation and growth, which typically occur in first-order

transitions. (ii) $c(4 \times 4)$ patches form in the middle of $(2 \times n)$ terraces (i.e. the upper terraces of relatively smooth S_A steps). (Note that the apparent darker patches are in the same atomic layer with the surrounding $(2 \times n)$ regions.) However, the density of the $c(4 \times 4)$ patches close to S_B steps is markedly lower than that far from the steps, subsequently forming striped areas (so-called denuded zones) along S_B steps. The $(n \times 2)$ terraces

(i.e. the upper terrace of S_B steps) consistently appear free of $c(4 \times 4)$ patches, implying that their denuded-zone width is larger than their terrace size. (iii) The growth rate of the $c(4 \times 4)$ phase is roughly proportional to the remaining $(2 \times n)$ areas and, therefore, obeys first-order kinetics. The above observations can be clarified in the following speculative scenario: the slow conversion of a parallel ad-dimer (i.e. the primary structure element in $c(4 \times 4)$ [22]) from an ordinary dimer dominates the transition rate due to a large activation energy. A parallel ad-dimer, once generated, migrates on the surface and incorporates itself into existing $c(4 \times 4)$ domains as well as steps [30]. The low $c(4 \times 4)$ patch density and large denuded zones around S_B steps imply that a parallel ad-dimer has a relatively high surface diffusion rate and a larger sticking coefficient at S_B steps than that at S_A steps [31]. The width of a denuded zone around S_B steps is larger on $(n \times 2)$ terraces than on $(2 \times n)$ terraces, indicating that the diffusion of a parallel ad-dimer, resembling an ordinary dimer, is markedly faster along dimer rows than perpendicular to them [31]. The parallel ad-dimers generated on $(n \times 2)$ terraces reach the S_B steps and become incorporated before there is any likelihood of them colliding with each other, thereby leading to island-free terraces. By assuming that the STM tip induces the generation of parallel ad-dimers, this scenario also corresponds to the formation process in Fig. 4. As Fig. 4 shows, the tip generates parallel ad-dimers much faster than does thermal activation. Therefore, with a fixed diffusion coefficient, denuded-zone widths on both the (2×1) and (1×2) terraces are considerably reduced.

Minimization of the free energy causes a surface reconstructive transition from an initial to a final state with different symmetries over time. This is a process of attaining equilibrium. Accordingly, the transitions $(2 \times 1) \rightarrow (2 \times n) \rightarrow c(4 \times 4)$ occur because the initial (2×1) (formed by a quenching effect) and the intermediate $(2 \times n)$ structures are not in true thermodynamic equilibrium at low temperatures. Tersoff [32] obtained a small energy (~ 0.05 eV per (1×1) unit cell relative to (2×1)) for the $(2 \times n)$ phase [32]. Uhrberg et al. [22] calculated the total energy of the $c(4 \times 4)$ structure. According to their results, the energies of parallel

ad-dimer and mixed ad-dimer structures are ~ 0.1 eV per (1×1) cell larger than that of (2×1) . They also suggested that the mosaic mixture of the two structures (as confirmed by the STM images) may have a lower energy than either of the two pure structures by balancing the strain energy and the dangling-bond energy. In addition, another work [33] demonstrated that a modest strain may drive a surface reconstruction. The fact that the strains associated with various dimer arrangements can easily be temperature-dependent raises the possibility that the strain energies at low temperatures tip the balance of the two energies in (2×1) in favor of $(2 \times n)$ and $c(4 \times 4)$. Further investigations are necessary to establish the temperature-dependent total energies of these phases and the driving forces for the transitions.

Acknowledgements

The authors would like to thank T.C. Chiang, C.C. Huang, T.M. Wu and H.F. Meng for valuable discussions, as well as the National Science Council of Taiwan for financial support under Contract No. NSC85-2112-M009-024.

References

- [1] V.G. Lifshits, A.A. Saravn, A.V. Zotov, *Surface Phases on Silicon*, Wiley, Chichester, 1994, and references therein
- [2] J.A. Kubby, J.J. Boland, *Surf. Sci. Rep.* 26 (1996) 61
- [3] O.L. Alerhand et al., *Phys. Rev. Lett.* 64 (1990) 2406
- [4] J. Wang, T.A. Arias, J.D. Joannopoulos, *Phys. Rev. B* 47 (1993) 10497
- [5] J.A. Martin, D.E. Savage, W. Montz, M.G. Lagally, *Phys. Rev. Lett.* 56 (1986) 1936
- [6] F.K. Men et al., *Phys. Rev. B* 52 (1995) R8650
- [7] T. Aruga, Y. Murata, *Phys. Rev. B* 34 (1986) 5654.
- [8] T. Sakurai et al., *Prog. Surf. Sci.* 33 (1990) 3
- [9] H. Feil et al., *Phys. Rev. Lett.* 69 (1992) 3076
- [10] K.E. Johnson, P.K. Wu, M. Sander, T. Engel, *Surf. Sci.* 290 (1993) 213
- [11] Y. Wei, Y. Hong, I.S.T. Tsong, *Appl. Surf. Sci.* 92 (1996) 491
- [12] Z. Zhang, M.A. Kulakov, B. Bullemer, *Surf. Sci.* 369 (1996) 69
- [13] D-S Lin, P.H. Wu, unpublished
- [14] A.J. Hoven et al., *J. Vac. Sci. Technol. A* 8 (1990) 207

- [15] H. Niehus, U.K. Kohler, M. Copel, J.E. Demuth, *J. Microsc.* 152 (1988) 735
- [16] H.J.W. Zandvliet, *Surf. Sci.* 377–379 (1997) 1.
- [17] H.C. Wang, R.F. Lin, X. Wang, *Phys. Rev. B* 36 (1987) 7712
- [18] R.N. Thomas, M.H. Francombe, *Appl. Phys. Lett.* 11 (1967) 108
- [19] T. Sakamoto et al., *Surf. Sci.* 86 (1979) 102
- [20] W.K. Liu, S.M. Mokler, N. Ohtani, B.A. Joyce, *Surf. Sci.* 264 (1992) 301
- [21] S. Nayak et al., *J. Crystal Growth* 157 (1995) 168.
- [22] R.I.G. Uhrberg, *Phys. Rev. B* 46 (1992) 10251
- [23] T. Ide, T. Mizutani, *Phys. Rev. B* 45 (1992) 1447
- [24] F.K. Men, J.L. Erskine, *Phys. Rev. B* 50 (1994) 11200
- [25] T. Takaoka, T. Takagaki, Y. Igari, I. Kusunoki, *Surf. Sci.* 347 (1996) 105
- [26] M. Sturmat, R. Koch, K.H. Reider, *Phys. Rev. Lett.* 77 (1996) 5071
- [27] Y. Wang, R.J. Hamers, *Phys. Rev. Lett.* 74 (1995) 403
- [28] Z. Zhang, M.A. Kulakov, B. Bullemer, I. Eisele, A.V. Zotov, *J. Vac. Sci. Technol. B* 14 (1996) 2684
- [29] It is known that the Si(100)-(2×1) surface is easily contaminated at room temperature. However, our samples were kept at elevated temperatures. At these temperatures, Si etching, presumably mainly by residual O₂, certainly occurs. However, etching by O₂ at <10⁻⁸ Torr and >600°C leads only to step retraction due to the fact that diffusion of DVs to steps occurs faster than the creation of new vacancies [11]. Also, sublimation proceeds at >825°C via the detachment of atoms from steps, as shown in M. Mundschau, E. Bauer, W. Teheps, *Surf. Sci.* 223 (1989) 413.
- [30] The incorporation of the parallel ad-dimer into c(4×4) regions requires the concerted removal of ordinary dimers, since the atomic density of the c(4×4) structure is lower than that of (2×1). This poses no difficulty in our model, since surface atoms are quite mobile at >590°C. The additional atoms simply diffuse and incorporate into step edges, leading to step advance (particularly the down step of a (n×2) terrace), as evident from the uneven size of two alternate terraces in Fig. 1h.
- [31] Y.-W. Mo, M.G. Lagally, *J. Crystal Growth* 111 (1991) 876
- [32] J. Tersoff, *Phys. Rev. B* 45 (1992) 8833
- [33] D. Vanderbilt, *Phys. Rev. B* 36 (1987) 6209